Lasers in Manufacturing Conference 2025

Scaling effects of fast laser drying processes in battery production

Delil Idris Demir[a], Mariam Saad[a], Samuel Moritz Fink[a]

[a]*Fraunhofer Institure for Laser Technology ILT, Steinbachstr. 15, 52074 Aachen, Germany*

Abstract

This study investigates the effects of laser drying on the quality of graphite-based lithium-ion battery anodes, using a water-based slurry of graphite, conductive carbon, carboxymethyl cellulose (CMC), and styrene-butadiene rubber (SBR). The slurry was coated onto copper foil using a roll-to-roll slot-die process and dried by either a convection oven or a laser module for comparison. Process parameters such as wet coating thickness (130 µm and 200 µm), web speed (1 m/min and 2 m/min), and drying temperature (70–110 °C) were systematically varied. Residual humidity and adhesion were evaluated using thermogravimetric analysis and adhesion testing, respectively. Results show that laser drying achieves up to 90% of the adhesion values obtained with conventional oven drying for thin coatings (130 µm) in less than half the drying time. Laser-dried electrodes also exhibit lower residual humidity compared to oven-dried benchmarks. However, higher evaporation rates and greater coating thicknesses promote binder migration and reduce adhesion, highlighting the need for precise control of drying parameters. Overall, laser drying demonstrates significant potential for efficient, high-quality electrode manufacturing, particularly for thinner coatings.

Keywords: Laser drying; Electrode manufacturing; Binder migration; Lithium-ion battery; Residual humidity; Adhesion; Scaling effects

1. Motivation

Addressing climate change requires advances in renewable energy and energy storage technologies. Lithium-ion batteries (LIBs), widely used in electronics and electric vehicles for their high energy and power densities, are increasingly in demand. This growth, along with changing geopolitical conditions, makes efficient and low-energy manufacturing processes essential. Electrode drying is among the most energy-intensive steps in LIB production, with conventional convection furnaces operating on 90% natural gas and accounting for up to 47% of the total energy consumption in battery manufacturing (Degen & Schütte, 2022) (Liu, Zhang, Wang, & Wang, 2021). Laser-based drying has emerged as a promising alternative, offering rapid, localized heating of the electrode active material and reducing energy consumption by up to 50 percent (Vedder, et al., 2016). However, challenges remain, such as managing temperature gradients and ensuring uniform drying to prevent defects like cracks or delamination. Optimizing laser drying is thus vital for the sustainable, efficient, and high-quality production of LIB electrodes.

2. Material and methods

The electrode investigated in these experiments serves as the anode and is composed of the active material graphite, conductive carbon, and the binders carboxymethyl cellulose (CMC) and styrene-butadiene rubber (SBR). Deionized water acts as the solvent to create the slurry. The composition of the used slurry is shown in Table 1. To achieve a homogeneous material distribution, the process begins with mixing the dry components (graphite, conductive carbon, and CMC) in an Eirich EL1 laboratory mixer for 30 minutes. In a separate step, the liquid components (deionized water and SBR) are also mixed for 30 minutes. The liquid mixture is then added to the dry mixture and mixed for an additional 120 minutes to form a homogeneous slurry. The final step is degassing the slurry in a vacuum container to remove air bubbles.

Table 1: Electrode slurry composition

Material	Material specification	Mass wet [wt.-%]	Mass dry [wt.-%]
Graphite	SIGRACELL GAM-AR20B	37.2	93.0
Conductive carbon	C-NERGY SUPER C65 Conductive Carbon Black	1.2	3.0
Carboxymethyl cellulose (CMC)	MAC500LC	0.8	2.0
Styrene-butadiene rubber (SBR)	BM-451B	0.8	2.0
Deionized water (DI-water)	-	60	-

The experiments are conducted using a Coatema Smartcoater SC32 roll-to-roll electrode manufacturing machine. The slurry is continuously coated onto a copper current collector substrate with a slot-die to achieve a specified thickness. After coating, the electrode is passed through a convection oven module and a laser module to remove the solvent from the coating. The convection oven and the laser module are used separately to compare laser drying with oven drying as a benchmark.

The convection oven heats the entire electrode, providing uniform air temperature that causes the solvent to evaporate gradually from the coating. This method relies on convective heat transfer, where hot air flows over the electrode surface, promoting solvent evaporation and removal. Temperature, airflow rate, and drying time in the oven are controlled to ensure consistent drying and to prevent defects such as cracking or delamination in the electrode film.

The laser drying module is set up as shown in Figure 1. A Laserline LDM6000 continuous wave 980 nm diode laser with a maximum power output of 6 kW is fiber-coupled with a Laserline fixed lens system. The fixed lens system has a working distance of 1165 mm and produces a laser spot measuring 466 × 280 mm². The laser spot features a homogeneous top-hat intensity distribution.

An Optris Xi 400 thermal camera is used to measure the hottest area within the processing are which is irradiated by the laser. This camera is integrated into a closed-loop temperature control system that adjusts the laser power output and regulates the surface temperature. The laser radiation is absorbed by the active material particles in the coating, resulting in rapid heating of the particles and therefore the coating and evaporation of the solvent. An air knife produces an airflow across the surface of the drying area to remove the evaporated solvent. This airflow moves the solvent vapor away from the electrode surface and prevents vapor from condensing back onto the coating. The evaporated solvent is removed from the module by a vapor extraction system, which transports the vapor out of the drying chamber. This arrangement of heating, airflow, and vapor extraction supports uniform drying of the electrode and helps prevent defects such as uneven drying, crack formation, or surface contamination.

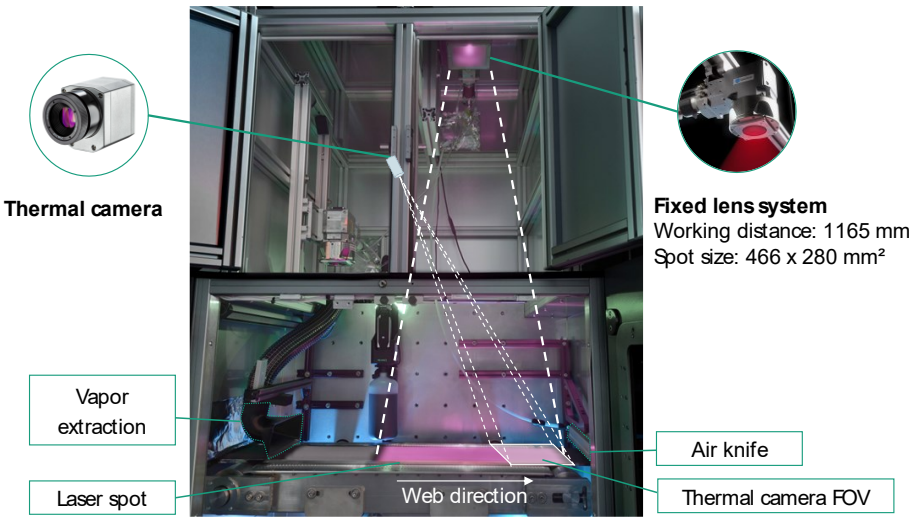

Figure 1: Laser drying module setup

The residual humidity of the dried electrodes is analyzed after the drying process. Circular samples with a diameter of 40 mm are cut out of from the electrode and analyzed using a RADWAG MA 50/1.X2.IC.A.WH thermogravimetric analyzer (TGA). To determine the residual humidity of the samples, the uncoated substrate mass is measured and subtracted from the total electrode mass, to obtain the coating mass.

After laser drying, the electrodes are weighted for their mass M_{laser}, and their residual humidity is measured using TGA. During TGA analysis, all remaining solvent is removed, yielding the dry mass M_{dry}. The wet coating mass M_{wet} is calculated based on the mixing ratio. The residual humidity is calculated as follows:

$$Residual\ humidity = \frac{M_{laser} - M_{dry}}{M_{wet}} \times 100\ \% \qquad (1)$$

The measurement of the adhesion (between the coating and the substrate) and cohesion (within the coating itself) is illustrated in Figure 2. Adhesive tape is applied to both the upper and lower plungers, and the electrode sample is placed on the tape attached to the lower plunger. During the measurement process, the upper plunger is pressed onto the lower plunger with a compression stress of 600 kPa and a compression velocity of 0.75 mm/min. The dwell time of 30 seconds enables the tape to grip the electrode and compresses the electrode slightly, similar to the calendering process in industrial production, which enhances adhesion. The pull-off is performed at a velocity of 100 mm/min. Since cohesion is typically higher than adhesion for graphite electrodes, cohesive failures are uncommon and indicate mechanical damage during calendering or the use of materials unsuitable for this application. Adhesive failures are used to investigate inhomogeneous binder distribution, insufficient binder content, or binder migration.

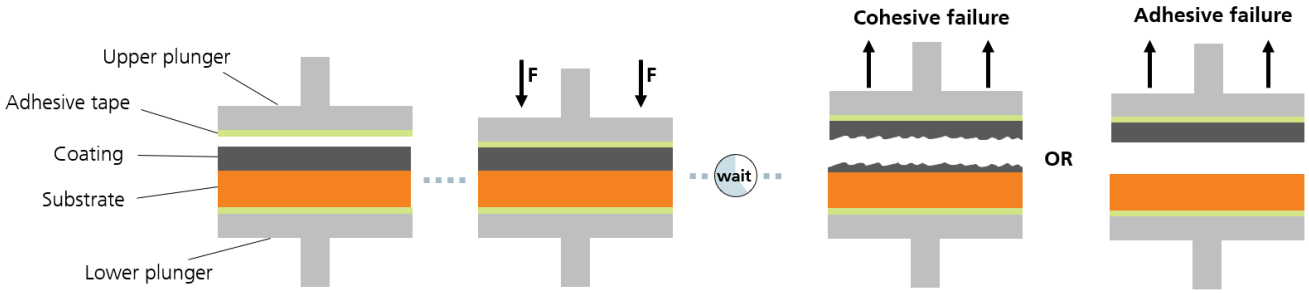

Figure 2: Adhesion and cohesion testing setup

3. Results and discussion

To investigate the effects of wet coating thickness, drying interaction time, and drying temperature on the electrode quality, laser drying experiments are conducted. The variation of the parameters wet coating thickness, web speed and drying temperature, are shown in Table 2. The results are compared to a convection-based oven benchmark. The benchmark electrode is produced with a wet coating thickness of 200 µm, a web speed of 1 m/min, and a convection air temperature of 150 °C. Although the benchmark uses convection drying at a higher air temperature, it provides a reference to quantify the performance of the different laser drying setups.

The standard drying temperature for laser drying of the anodes is 90 °C, based on preliminary tests. To assess the effect of electrode temperature during the laser drying process on electrode quality, lower (70 °C) and higher (110 °C) drying temperatures are also tested. Web speeds of 1 m/min and 2 m/min are used to create different interaction times, resulting in varying evaporation rates. These parameters are evaluated for wet coating thicknesses of 130 µm and 200 µm.

Table 2: Process parameter overview

Sample ID	Setup	Wet coating thickness h_{wet} [µm]	Web speed [m/min]	Interaction time [s]	Drying temperature [°C]
B1	Convection oven benchmark	200	1	60	150 (convection)
A1	Laser drying	130	1	28	70
A2	Laser drying	130	1	28	90
A3	Laser drying	130	1	28	110
A4	Laser drying	130	2	14	70
A5	Laser drying	130	2	14	90
A6	Laser drying	130	2	14	110
A7	Laser drying	200	1	28	70
A8	Laser drying	200	1	28	90
A9	Laser drying	200	1	28	110
A10	Laser drying	200	2	14	70
A11	Laser drying	200	2	14	90
A12	Laser drying	200	2	14	110

In Figure 3, thermal images of the laser drying process are presented for samples A1 and A8. The hotspot, which is used for closed-loop temperature control is indicated in the figure. The temperature distribution can indicate various coating defects. Streaks in the coating can result from slot-die nozzle blockages, leading to areas with reduced coating thickness. Due to the uniform laser intensity in the drying area, these thinner regions dry more quickly and can reach higher temperatures, increasing the risk of overheating. The temperature control system mitigates this risk by adjusting the maximum temperature on the electrode surface. Other challenges include point defects, which can occur when the substrate foil comes into contact with the underlying stainless steel floating gas table, transferring heat to the electrode in localized areas.

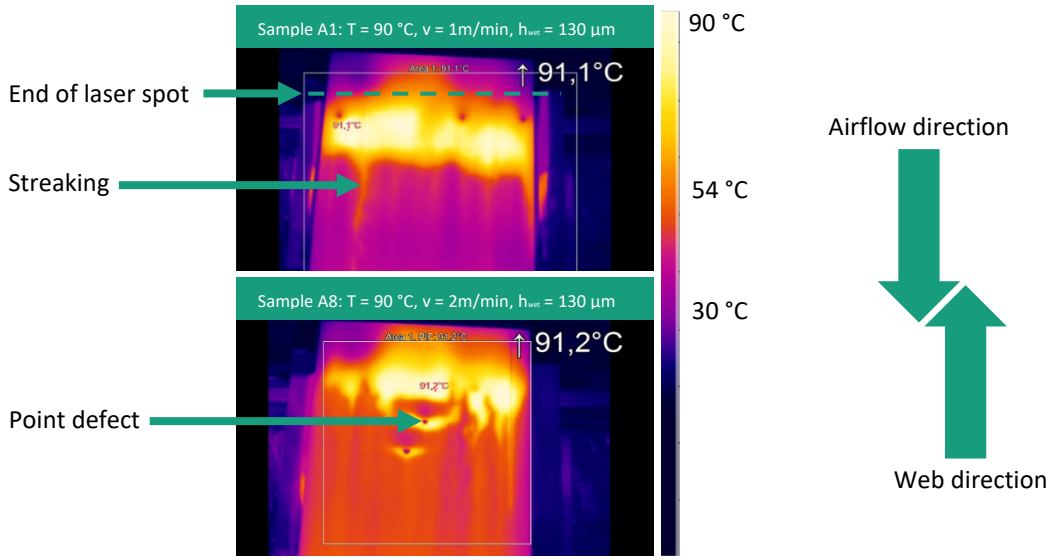

Figure 3. Thermographic temperature control imaging

In Figure 4 photographs of the laser dried samples A1 and A11 are depicted. Both samples are processed at a temperature of 90 °C, but differ in wet coating thickness and web speed. Sample A1 exhibits a uniform surface with no visible defects. Additional adhesion measurements are conducted to assess binder migration and mechanical stability.

In contrast, the surface of sample A11 displays cracks along the length of the electrode. These cracks are likely caused by a skin effect, which results from a high evaporation rate and the formation of a dried surface with reduced active material porosity. Lower porosity impedes the escape of evaporated solvent, leading to a buildup of solvent vapor pressure beneath the surface. As this pressure increases, it can cause the dried surface to crack.

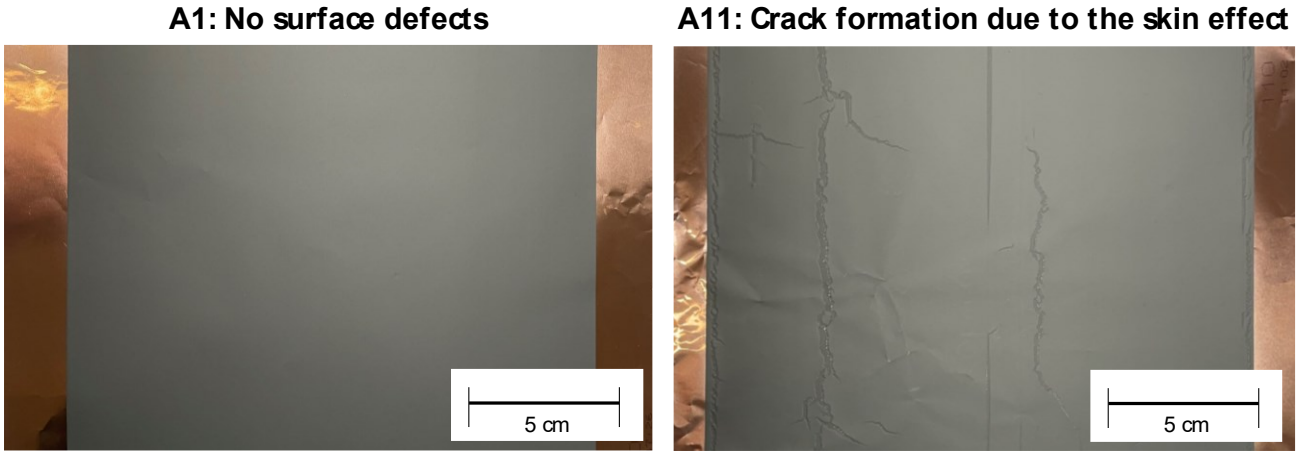

Figure 4: Visual inspection of samples A1: T = 90 °C, v = 1m/min, h_{wet} = 130 µm (left) and A11: T = 90 °C, v = 2m/min, h_{wet} = 200 µm (right)

The residual humidity analysis of the samples A1 to A6 are compared to the benchmark B1 in Figure 5 (left). These samples were prepared with a wet coating thickness of 130 µm, web speeds of 1 and 2 m/min, and were laser dried at 70 °C, 90 °C, and 110 °C, respectively. The oven-dried benchmark (B1) shows a higher residual humidity of 1 ± 0.9 wt.% compared to the laser-dried samples. The high standard deviation in the samples is likely due to variations in the slot-die coating process, which produces a wet coating thickness variation of approximately ± 10 µm (± 8%) and is determined with a Keyence CL3000 system. Since temperature control targets the hottest spot on the electrode and the laser intensity is homogeneous across the area, thinner regions dry faster and thus reach higher temperatures. This contributes to the higher standard deviation in residual humidity.

The graph shows that for a wet coating thickness of 130 µm, lower drying temperatures in samples A1 and A4 result in the lowest residual humidity for both web speeds. Increasing the drying temperature to 90 °C and 110 °C leads to higher residual humidity in the electrodes. A possible explanation is that higher drying temperatures cause a rapid temperature increase and higher evaporation rates at the beginning of the drying process. This can create a dried surface with lower porosity and remaining solvent near the substrate-coating interface. Reduced porosity hinders capillary transport of the solvent to the surface, resulting in higher residual humidity. Lower drying temperatures are associated with a more uniform drying process and prevent thermal damage of the surface.

The residual humidity analysis for samples A7 to A12 is compared to the benchmark B1 in Figure 5 (right). These samples are prepared with a wet coating thickness of 200 µm, web speeds of 1 and 2 m/min, and are laser dried at 70 °C, 90 °C, and 110 °C, respectively. The oven-dried benchmark (B1) again shows a higher residual humidity of 1 ± 0.9 wt.% compared to most of the laser-dried samples. Electrodes with a wet coating thickness of 200 µm require more energy to remove the solvent than those with a thickness of 130 µm. The high standard deviation in sample A10 is likely caused by the slot-die coating process, which produces a wet thickness variation of approximately ± 10 µm (± 4%). At the higher web speed of 2 m/min, the energy input is insufficient for complete drying. Thickness variation also significantly affects the standard deviation in residual humidity.

All other samples show a lower standard deviation than samples A1 to A6, and their residual humidity values are below the mean of the oven benchmark. Due to the standard deviation and the similarity in mean residual humidity, no further conclusions can be drawn regarding differences in drying behavior.

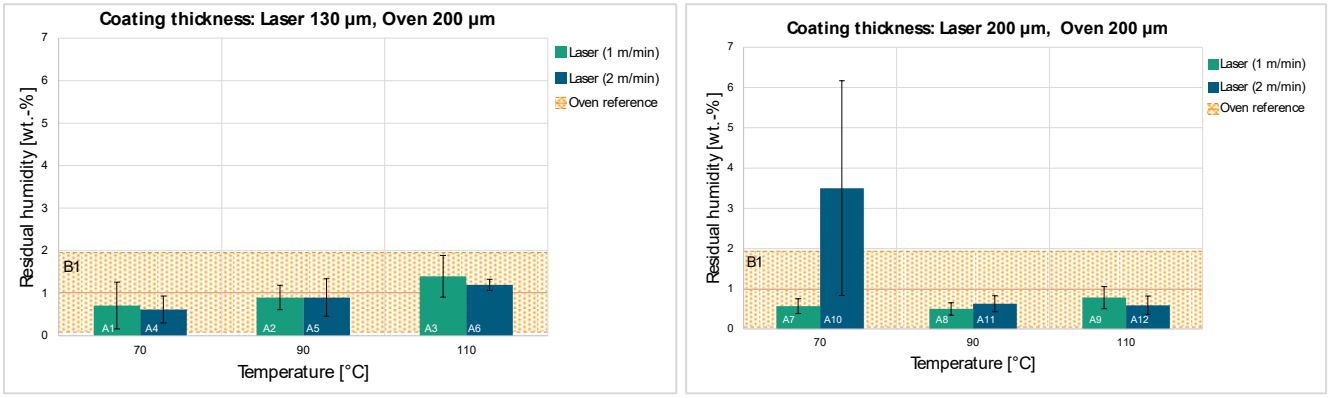

Figure 5: Residual humidity of samples with wet coating thickness of 130 µm (left) and 200 µm (right)

The adhesion analysis of the samples A1 – A6 is compared to the benchmark B1 in Figure 6 (left). The oven-dried benchmark (B1) shows a measured adhesion of 482 ± 51 kPa, which is higher than the adhesion values of the laser-dried samples A1 to A6. High adhesion is desirable to prevent delamination of the active material coating from the current collector substrate during further processing. The high standard deviation observed in the samples is likely due to variations in the slot-die coating process, which results in a wet coating thickness variation of ±8%. Among the laser-dried samples, A1 exhibits the highest mean adhesion value at 434 ± 46 kPa, reaching 90% of the oven benchmark. The data indicate that increasing the drying temperature leads to a decrease in mean adhesion. This effect can be explained by the steeper temperature ramp and higher solvent evaporation rates at elevated drying temperatures. High evaporation rates during the final stages of drying can cause binder migration within the active material coating (Kumberg, et al., 2019). This explanation is further supported by the comparison of different web speeds, since higher web speeds produce higher evaporation rates due to the shorter interaction time between the coating and the laser spot.

The adhesion analysis of the samples A7 – A7 is compared to the benchmark B1 in Figure 6 (right). The oven-dried benchmark (B1) again shows a measured adhesion of 482 ± 51 kPa, which is higher than the adhesion values of the laser-dried samples A7 to A12. The standard deviation in these samples is likely due to the slot-die coating process, which has a wet coating thickness variation of ±4% and results in varying evaporation rates because of the homogeneous laser intensity in the drying area. Among the laser-dried samples, A9 shows the highest mean adhesion value at 315 ± 35 kPa, reaching 65% of the oven benchmark and displaying a lower standard deviation. All samples in this group exhibit lower adhesion than the oven reference. Furthermore, samples A7 to A12 with a wet coating thickness of 200 µm exhibit lower adhesion than samples A1 to A6, supporting the observation that shorter interaction times result in reduced adhesion. Additionally, higher wet coating thicknesses require more energy for drying due to the greater total mass of active material and solvent. This increases evaporation rates, which can promote binder migration and thermal damage. Dry areas have a lower porosity than wet areas. Therefore a dry surface causes lower porosity at the surface and hinders solvent transport from deeper regions near the substrate-coating interface to the electrode surface.

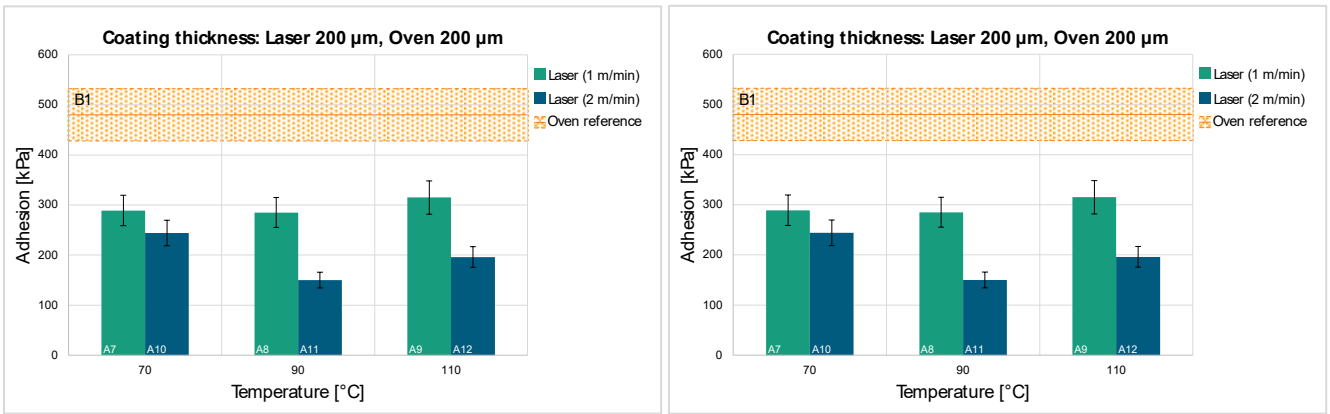

Figure 6: Adhesion of samples with wet coating thickness of 130 µm (left) and 200 µm (right)

4. Summary

The scaling effects of the laser drying process demonstrate the significant influence of wet coating thickness, process time, and evaporation rate on electrode quality. High adhesion values of up to 90 percent of those achieved with conventional convection drying were obtained for electrodes with a 130 µm wet coating thickness. This contrasts with benchmarks using a 200 µm wet coating thickness. These high adhesion values were reached in less than half the process time required by conventional methods.

The results further indicate that higher evaporation rates and greater wet coating thicknesses lead to increased binder migration within the electrode. Binder migration can impact the uniformity and mechanical stability of the electrode, highlighting the importance of precise control over drying parameters. Additionally, electrodes dried with the laser process consistently show lower residual humidity compared to those produced by conventional drying.

References

Degen, F., & Schütte, M. (2022). *Life cycle assessment of the energy consumption and GHG emissions of state-of-the-art automotive battery cell production.* Journal of Cleaner Production, Volume 330, 1 January 2022, 129798.

Liu, Y., Zhang, R., Wang, J., & Wang, Y. (2021). *Current and future lithium-ion battery manufacturing.* iScience, 24(4), 102332.

Vedder, C., Hawelka, D., Wolter, M., Leiva, D., Stollenwerk, J., & Wissenbach, K. (2016). *Laser-based drying of battery electrode layers Available.* ICALEO 2016: 35th International Congress on Applications of Lasers & Electro-Optics

Kumberg, J., Müller, M., Diehm, R., Spiegel, S., Wachsmann, C., Bauer, W., Scharfer, P., Schabel, W. (2019). *Drying of Lithium-Ion Battery Anodes for Use in High-Energy Cells: Influence of Electrode Thickness on Drying Time, Adhesion, and Crack Formation.* Energy Technol., 7: 1900722.